Preparation and characteristics of seeded epitaxial $(Sr,Ba)Nb_2O_6$ optical waveguide thin films using sol-gel method

Junmo Koo, Jae Hyeok Jang, and Byeong-Soo Bae
Laboratory of Optical Materials and Coating (LOMC), Department of Materials Science and Engineering, Korea Advanced Institute of Science and Technology (KAIST), Taejon 305-701, Korea

(Received 10 October 2000, accepted 30 October 2000)

Highly *c*-axis-oriented $(Sr,Ba)Nb_2O_6$ (SBN) films were grown on a seeded MgO(100) substrate via sol-gel method. The substrate was preseeded with epitaxial islands of SBN made by breaking up a continuous film into single-crystal islands by pores. Since the number of epitaxial nuclei was increased at the interface between the film and the substrate, the film on a seeded substrate had better highly orientation than that on unseeded substrate. The film having low Sr content exhibited better epitaxial growth because of the distorted unit-cell network and the change of lattice parameters of SBN thin film. For obtaining excellent optical properties, SBN:75 film was prepared on MgO substrate with SBN:25 composition seed layer. Because of low birefringence of refractive indices in the film having high Sr content, the optical scattering loss by the anisotropy of refractive indices was suppressed.

I. INTRODUCTION

Strontium barium niobate ($Sr_xBa_{1-x}Nb_2O_6$, referred to as SBN:100*x*, where $0.25 \leq x \leq 0.75$) is currently being investigated as a potential ferroelectric material for many microdevice applications, such as pyroelectric infrared detectors, electro-optic modulators, holographic storage, and beam steering, because of its large pyroelectric coefficient, excellent piezoelectric and electro-optic properties, and photorefractive sensitivity.[1–4] Compared with other well-known ferroelectric materials, SBN has an extremely high electro-optic coefficient, for example, the figure of merit is more than 50 times higher than that of $LiNbO_3$, offering the possibility of much smaller devices.[3] SBN is a solid solution between $BaNb_2O_6$ and $SrNb_2O_6$ phases with a tetragonal tungsten bronze (TTB) structure, and its physical properties vary with its composition.[5] These properties and their applications have been investigated mainly for single crystals and polycrystalline ceramics. However, the demand for thin film processing has increased due to the development of electronic and optical integrated devices. SBN thin films, especially highly *c*-axis-oriented SBN thin films, are desired for optical applications, such as electro optic properties, photorefractive, and nonlinear optical applications because these applications can take full advantage of SBN films' ferroelectricity.[6–8] There are several kinds of fabrication techniques for thin films such as radio frequency (rf) sputtering, metalorganic chemical vapor deposition (MOCVD), the sol-gel method, and pulsed laser depositions. Among these, the sol-gel process has been developed for ferroelectric thin film processes due to excellent homogeneity, ease of chemical composition control, high purity, low processing temperature, and film uniformity over a large area. Therefore, many papers recently reported on the synthesis of SBN thin films by using the sol-gel method.[4,8–10] However, it was hard to obtain fully densified and oriented SBN thin films, and the quality of sol-gel-derived films was not better than the vacuum-deposited films prepared by pulsed laser deposition[6] or metalorganic chemical vapor deposition.[7] Generally, the heterogeneous nucleation at the interface between the film and the lattice-matched substrate would lead to the formation of highly preferred orientation or epitaxial thin films. The vacuum-deposited films are grown *in situ* with the following mechanisms: condensation of vapor atoms and ions on the substrate surface, nucleation, and growth. Nucleation initiated on the surface of the substrate having a lattice match with the film leads to epitaxial growth. In the case of the sol-gel derived film, the epitaxial growth is related to the crystallization of the solid amorphous film prepared by coating and drying. The nuclei form not only within the bulk but also at the interface between the film and the substrate for the sol-gel process. Thus, in the sol-gel method it is very difficult to control the nucleation rate and the location of the nuclei during the crystallization of amorphous film. In addition, since the crystal and optical studies of SBN single crystal has focused on the material with mainly SBN:60 composition because of its congruent

melt composition ($x = 0.6$),[5] the characteristics of SBN thin films have also dealt with that composition. Recently, although Hirano and *et al.* synthesized the highly *c*-axis-oriented SBN:50 thin films on an MgO(100) substrate by sol-gel method;[8] the other compositions of the film have not been studied.

So far, there have been many reports on epitaxially growing the oxides on lattice-matching substrates using a seeded thin film growth method.[11–14] The method originates from two mechanisms: first, a microstructural instability phenomenon where a polycrystalline film breaks into single-crystal islands during grain growth;[11] second, a continuous film containing an equilibrium area fraction of holes and/or pores grows together to cause the film to break up into single-crystal islands.[14] Each mechanism can be applied to different systems, such as ZrO_2/Al_2O_3 and $PbTiO_3/SrTiO_3$ respectively, according to the difference of crystal structures and lattice parameters between the film and the substrate.

In the previous study, we obtained the fully densified SBN thin films on MgO(100) substrate having high *c*-axis orientation using the two-step heating process.[15] In the present study, we enhanced the orientation of the sol-gel-derived thin films on MgO(100) substrate with various compositions using a seeds layer. We also characterized optical properties of the films.

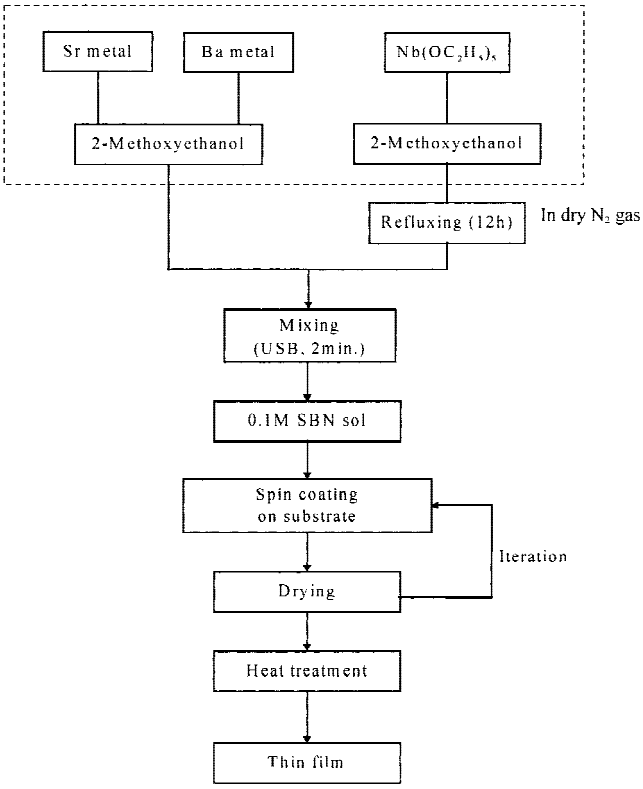

FIG. 1. Flow chart for fabrication of SBN thin films.

II. EXPERIMENTAL PROCEDURE

Three compositions investigated in the present work are: $x = 0.25$, 0.60, and 0.75 in the general chemical formula $Sr_xBa_{1-x}Nb_2O_6$. Strontium metal, barium metal (Aldrich Chemical), and niobium ethoxide (Aldrich Chemical) were used as the starting agents. The solvent used was 2-methoxyethanol (Aldrich Chemical), a common solvent for many sol-gel-prepared ferroelectric thin films like (Pb,La)(Ti,Zr)O_3 (PLZT) system because it stabilizes a solution against moisture.[9,16] Since an oxygen atom of the methoxyethoxy group has more negative partial charge than that of the ethoxy group in ethanol, this property makes 2-methoxyethanol a better nucleophilic solvent than ethanol.[9] Thus, the solution can be stored for several months without any suspended particles. Details of the procedure for preparing the precursor solution are shown in Fig. 1. Strontium metal and barium metal, corresponding to the desired stoichiometric ratio of the SBN, were dissolved in 2-methoxyethanol and refluxed at 120 °C for 6 h. This solution was then heated at 80 °C for 6 h to distill undesired organic compounds. A niobium solution was made with a similar process. The final solution, which had a concentration of 0.1 M, was clear brown. Each solution was mixed using an ultrasonic machine for 1 min before coating. The mixed solution was then spin-coated at 2000 rpm for 30 s on a MgO(100) single-crystal substrate. Transparent MgO single crystal shows good lattice matching with SBN crystal, which provides a possibility to grow an epitaxial SBN layer.[6–10] Also, because the refractive index of MgO is lower than SBN, SBN thin films on MgO substrates can be fabricated as planar optical waveguides.

After air drying for 5 min, the green film was dried at 180 and 360 °C for 10 min on a hot plate. One coating yields a film thickness of about 600 Å. This procedure was repeated until the desired thickness was obtained. The films were crystallized at 900 °C for 1 h using a modified heating schedule, i.e., two-step heating process. The two-step heating process applied an additive heat-treatment before crystallization. In the two-step heating process, the films were heated from room temperature to 550 °C with slow heating rate (= 2 °C/min) and maintained at 550 °C for 5 h to enhance the crystallization as well as the densification of the films. Then the temperature was raised to the crystallization temperature using same heating rate. The effect of the two-step heating process was described in another paper.[15] In addition, cooling rate was also maintained as 2 °C/min to prevent microcracks from thermal shock. For preparing a seeds layer on MgO(100) substrate, thinner films were prepared by a faster spin-coating at 3000 rpm, then heat-treated at 900 °C for 1 h to form isolated islands. The SBN film with seeded substrate can be obtained by over-coating these islands using multi-coatings.

Crystalline phase and microstructure of the films were characterized with an x-ray diffraction (XRD) analyzer (Rigaku, D/MAX-RC) and a scanning electron microscopy (Phillips, 535M). A diffractometer (Rigaku, D/MAX-IIIC) was employed for θ-2θ scans and pole figures. Atomic force microscopy (Park Scientific Instruments, Autoprobe 5M) was used to analyze surface morphologies and roughness of the thin films. Measurement of refractive indices of the films was performed by a prism coupler (Metricon, 2010) at wavelength of 632.8 nm. Optical propagation loss of the films was measured from an experimental set-up using a CCD camera.

III. RESULTS AND DISCUSSION

A. Preparation of epitaxial SBN thin film

Figure 2(a) shows AFM images of SBN seeds layer prepared on MgO(100) substrate. Many rectangular shaped islands with rounded corners were observed, and the size of islands was estimated for about 50 nm. The selected-area diffraction patterns (SADP) that include the islands with SBN:60 composition and the MgO substrate are shown in Fig. 2(b). Two sets of the diffraction patterns, which include a [001] pattern of the MgO substrate and a [001] pattern of the SBN islands, are indicated by the arrows. Since the lattice constant of SBN ($a_{SBN} \approx 12.4$ Å) is about three times lager than that of MgO ($a_{MgO} \approx 4.2$ Å), the 1 × 1 unit cell of SBN in the *c* plane corresponds to the equivalent 3 × 3 unit cells of MgO.[17] Both patterns showed good coincidence, known as the epitaxial orientation relationship of $\langle 100\rangle[001]_{SBN} \parallel \langle 100\rangle[001]_{MgO}$. These results mean that the SBN thin films were broken completely into the islands during the heat treatment, and these islands have an epitaxial relationship with respect to the MgO substrate, as mentioned above.

Figures 3 and 4 show XRD patterns and pole figures of SBN:60 thin films on unseeded and seeded MgO(100) substrates. All the films were crystallized with *c*-axis orientation consisting of single TTB SBN phase, regardless of the presence of a seeds layer, as shown in Fig. 3. However, the film on a seeded substrate [Fig. 4(a)] shows relatively sharp eight-equivalent peak-groups for SBN (00*l*) planes at $\alpha = 54.6°$ in SBN (211) pole figure plane, whereas the film on an unseeded substrate [Fig. 4(b)] has no definite peaks. The pole figure pattern in the film on a seeded substrate agrees with that of previous studies by other researchers.[6,8] These results indicate that the film on a seeded substrate has better lattice-matching than the film on unseeded substrate. Thus, the film on a seeded substrate has a single-crystal like texture consisting of a complete *z*-axis orientation and low-angle grain boundaries in the *x*-*y* plane. On the other hand, the film on an unseeded substrate is highly oriented polycrystalline film consisting of a complete

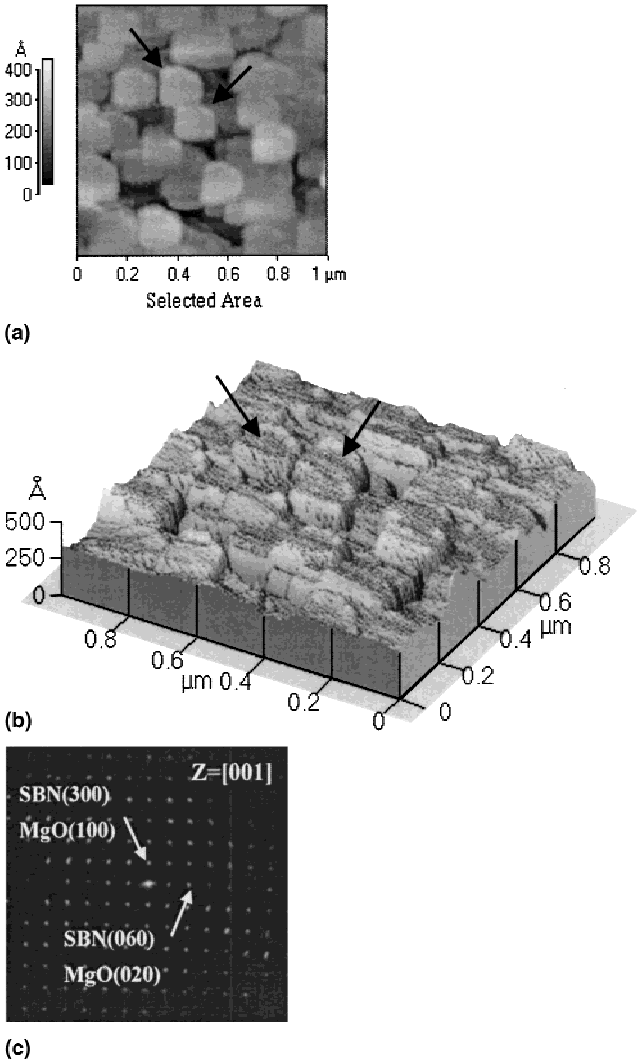

FIG. 2. (a) Plane-view and (b) 3D AFM images of SBN:60 seeds layer (≈400 Å) on MgO(100) substrate, and (c) selected-area diffraction pattern (SADP) of the (001) plane of SBN islands and MgO substrate.

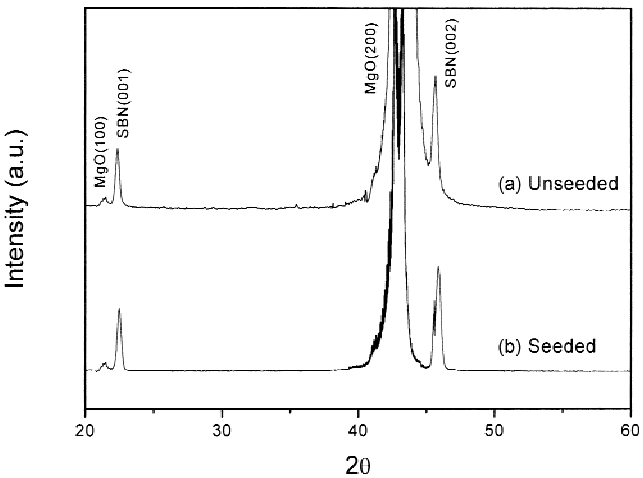

FIG. 3. XRD patterns of SBN:60 thin films (≈4000 Å thickness) on (a) unseeded and (b) seeded MgO substrates.

z-axis orientation and a random orientation in the *x*-*y* plane.[18] Figure 5 shows plane-view and cross-sectional SEM micrographs of SBN thin films on unseeded and seeded MgO(100) substrates. As shown in Figs. 5(a) and 5(c), spherical grains in the film on an unseeded substrate were observed to slightly coarsen (approximately 0.1 μm), and many grains were found in the whole cross section of the film, showing a small amount of grain boundaries. These phenomena mean that the film has distinct polycrystalline morphology, and the SBN nuclei form not only within the bulk, but also at the interface between the film and the substrate. On the other hand, for the seeded substrate, the film [Figs. 5(b) and 5(d)] showed smooth surface, as well as no crack and voids, and relatively few grains, except for grains found at the interface between the film and the substrate due to the SBN seeds layer. These results indicate that the nuclei initiated on the surface of the substrate would lead to the formation of highly preferred orientation or epitaxial thin films.

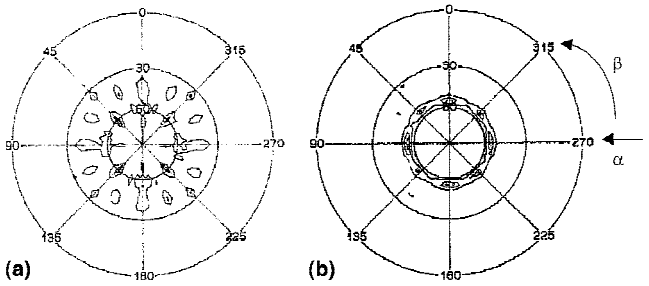

FIG. 4. XRD pole figure scans of SBN:60 thin films on (a) unseeded and (b) seeded MgO substrates [$2\theta = 27.7°$ for (211)].

Two different mechanisms for the formation of epitaxial thin films using a seeds layer were previously proposed by Miller[11] and Seifert.[14] Miller's model is applicable to a film/substrate system that has dissimilar crystal structure and larger interatomic spacings like the ZrO_2/Al_2O_3 system, contrary to Seifert's. Miller *et al.* proposed that highly oriented thin films can be formed by following sequential procedures: (i) formation of a continuous and dense polycrystalline thin film on a single-crystal substrate; (ii) growing of grains that have a special low energy orientation with the substrate by consuming neighbor grains that have either a small grain size or a high energy orientation with the substrate; (iii) formation of a layer having high orientation but isolated grains; (iv) epitaxial growth of an upper film by this seeds layer. On the other hand, Seifert *et al.* proposed that isolated epitaxial islands can be formed from a continuous epitaxial single-crystal thin film by the following procedures: (i) formation of a continuous and dense epitaxial thin film on a single-crystal substrate; (ii) growth of pre-existing holes and/or pores greater than a critical size when the film is thinner than the critical thickness; (iii) breaking up the film into epitaxial single crystal islands; (iv) epitaxial growth of the film by the seeds. Since the lattice mismatch [$m = |(a_{\text{film}} - 3 \times a_{\text{substrate}})/(3 \times a_{\text{substrate}})|$] between SBN and MgO is known to be about 1%, and there is a possibility that the SBN solution to contains some amount of micropores during mixing solutions, it appears that the islands in the present study were formed by the mechanism proposed by Seifert *et al.*

Figures 6 and 7 show XRD patterns and pole figures of SBN films on seeded MgO(100) substrates as a function

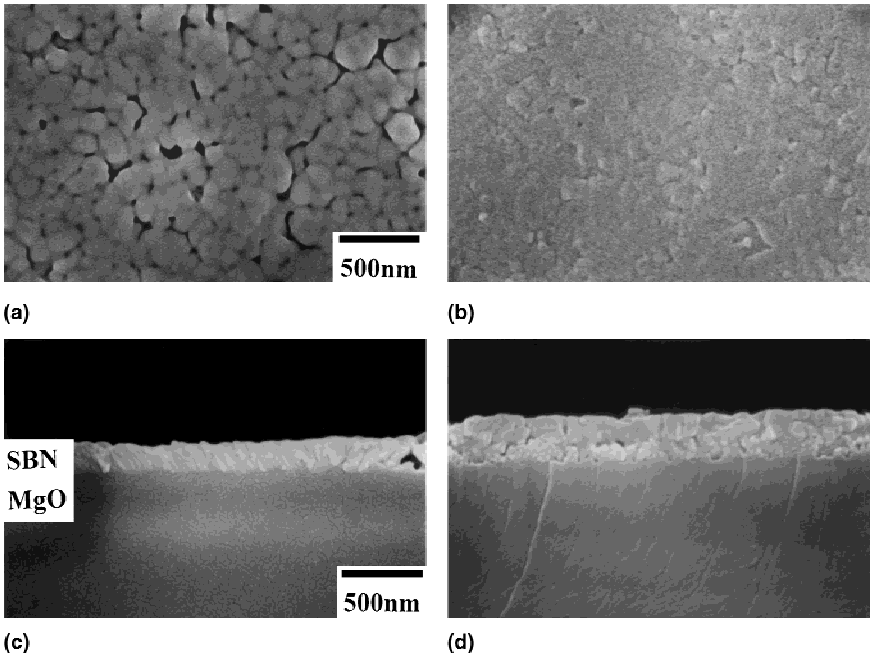

FIG. 5. Plane-view and cross-sectional SEM micrographs of SBN:60 thin films on (a,c) unseeded and (b,d) seeded MgO substrates, respectively.

of the film composition. The compositions of the isolated seeds layer were same with upper films. As shown in Fig. 6, all the films had the *c*-axis orientation consisting of single TTB SBN phase, regardless of the composition. However, in case of pole figures, eight-equivalent peak-groups of (00*l*) planes in the film having low Sr content were sharper than those in the film having high Sr content, as shown in Fig. 7. This result means that the epitaxy of SBN thin film was affected by the composition of the film. According to our previous study on structural behavior of SBN thin films,[15] there are two reasons for this phenomenon. First, the SBN thin film with higher Sr content has a more distorted unit-cell network. In the unit cell of TTB SBN phase, A_1 sites are occupied by only Sr^{2+} ions whereas A_2 sites are occupied by both Ba^{2+} and Sr^{2+} ions.[5] As the fraction of Sr^{2+} ion content increases, more Sr^{2+} ions occupy the A_2 sites and the A_1 sites become empty due to movement of Sr^{2+} ions. Then the lattice of SBN having higher Sr content will be more distorted.[15,17] Therefore, SBN:75 film presents a low quality of orientation, comparing with SBN:25 thin film. Second, the lattice parameters of SBN thin film vary with a change of composition. From the XRD measurement of sol-gel-derived SBN thin films from other papers,[15,19] while the calculated lattice constant along the *c* axis decreases from 3.941 to 3.832 Å as Sr content in the film composition increases, the lattice constant along *a* axis decreases from 12.5 to 12.37 Å. Therefore, the lattice mismatch between the film and the substrate increases from 1.07% to 1.31% as Sr content in the film increases, as shown in Fig. 8.

Since it is known that the SBN with high Sr content exhibits better electro-optic properties, as well as ferroelectric properties, the epitaxial SBN thin films having higher Sr content are required for optical waveguide applications.[20] As mentioned above, SBN:25 composition should be the content of an isolated seeds layer because the film having low Sr content presents a good epitaxy. Figure 9 shows pole figures of SBN:75 thin films on seeded MgO(100) substrates using the SBN:25 composition. Compared with the pattern in Fig. 7(c), the peak-groups of (00*l*) planes in the film become sharper, although it is not better than those in the SBN:25 thin film. Thus, the use of the SBN:25 composition seeds layer on MgO substrate is very effective for obtaining good epitaxial sol-gel–derived SBN thin films expected to have excellent optical properties. All the SBN thin films investigated for optical characterizations were prepared with a SBN:25 seeds layer.

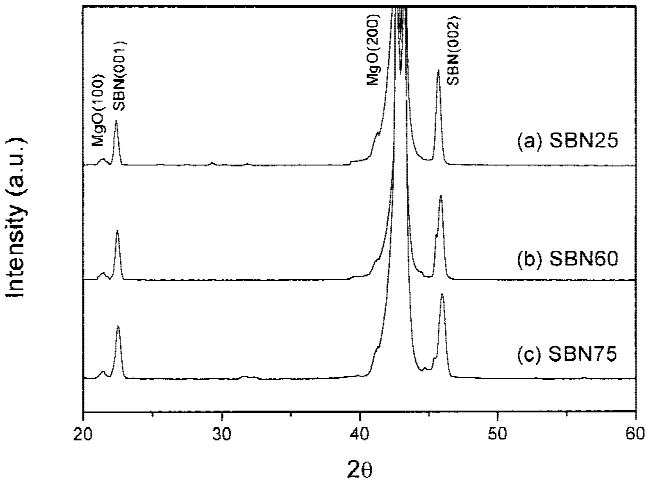

FIG. 6. XRD patterns of SBN thin films (≈4000 Å thickness) on seeded MgO substrates as a function of film composition: (a) SBN:25, (b) SBN:60, and (c) SBN:75.

B. Optical properties of epitaxial SBN thin films

Figure 10 shows the refractive indices of *c*-axis-oriented SBN films on the seeded MgO(100) substrates as a function of the composition. This result shows that SBN is optically uniaxial negative material ($n_o > n_e$). The ordinary refractive index n_o increases as Sr content in the film composition decreases due to an increase in the amount of BaO with higher refractive index. However, the extraordinary index n_e is more sensitive than the ordinary index to change in the film composition because n_e is affected by electronic and ionic polarization, the change in lattice parameter, and structure, whereas n_o is affected only by electronic polarization.[21] Thus, since the cause of the decrease in n_e with increasing Sr content in the film is very complicated, we don't know the principal factor exactly. However, the refractive indices of the films approach that of single crystal SBN, which reflects

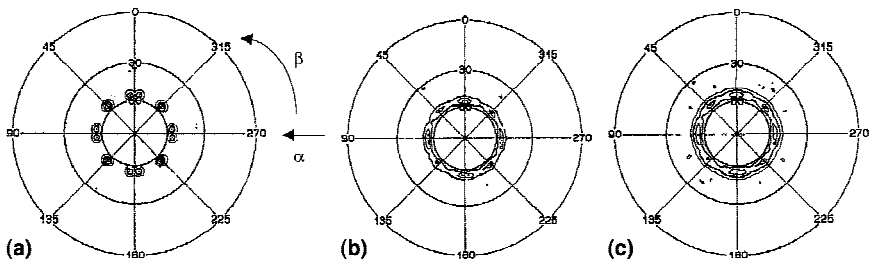

FIG. 7. XRD pole figure scans of SBN thin films on seeded MgO substrates as a function of film composition [2θ = 27.7° for (211)]: (a) SBN:25, (b) SBN:60, and (c) SBN:75.

that the films are fully densified.[4,21] It is also found that there is a difference between the refractive indices of the films on the SBN:25 composition seeded MgO(100) substrate and the unseeded substrate because the films on the seeded substrate may have multilayers consisting of upper film (SBN:100*x* composition) and seed islands (SBN:25 composition) with different indices. According to the result of our simulations, this multilayer does not affect the propagation of modes because of too thin a layer (≈400 Å) to guide a mode in the film. In addition, a birefringence, Δn ($= n_o - n_e$), decreases Sr content in the film composition, as shown in Fig. 10. The lower birefringence of the higher Sr content of SBN film prevents optical scattering from the anisotropic refractive indices. Generally, the optical scattering in the material is mainly due to a variation in refractive index of a birefringent material. Also, the high surface roughness of the film may produce a large variation in refractive index of the material.[22] Figure 11 is the plot of optical propagation loss and root-mean-square (rms) surface roughness of SBN thin films on seeded MgO(100) substrates. The optical propagation loss of the films decreases with an increase of Sr content, although the rms surface roughness of the films is not heavily varied, regardless of the composition. It appears that the surface roughness of all the films has constant value due to the absence of grain boundaries in the film. Therefore, the degree of birefringence becomes the dominant cause of the optical propagation loss in the SBN thin films, which have uniform surface roughness, regardless of composition.

IV. CONCLUSION

Highly *c*-axis-oriented SBN films were obtained with the sol-gel on a MgO(100) substrate using a seeded substrate. The isolated SBN seeds were formed by breaking

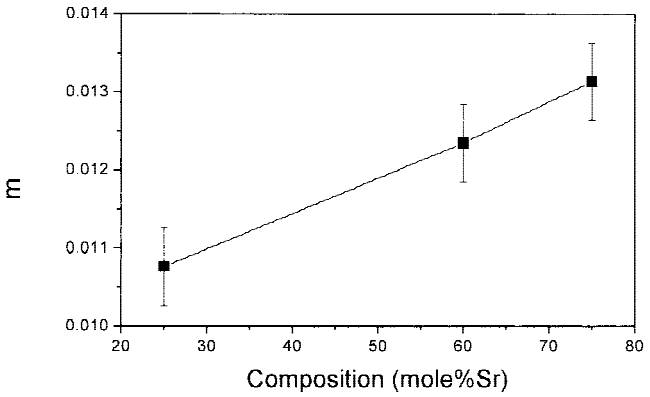

FIG. 8. Variation of the lattice mismatch m [$= |(a_{film} - 3 \times a_{substrate})/(3 \times a_{substrate})|$] between the SBN thin film and MgO substrate as a function of film composition.

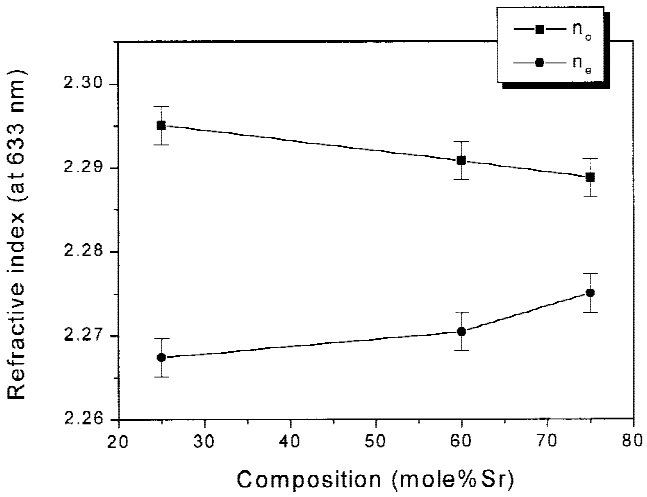

FIG. 10. Refractive indices of SBN thin films on SBN:25 composition seeded MgO substrate as a function of film composition.

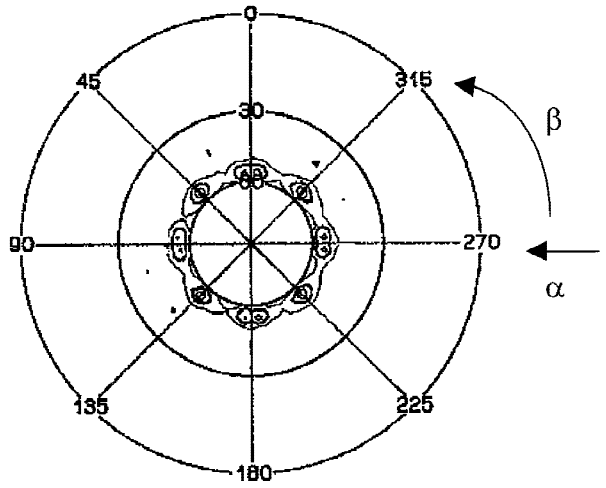

FIG. 9. XRD pole figure scans of SBN:75 thin films on MgO substrates using SBN:25 composition seed layer [$2\theta = 27.7°$ for (211)].

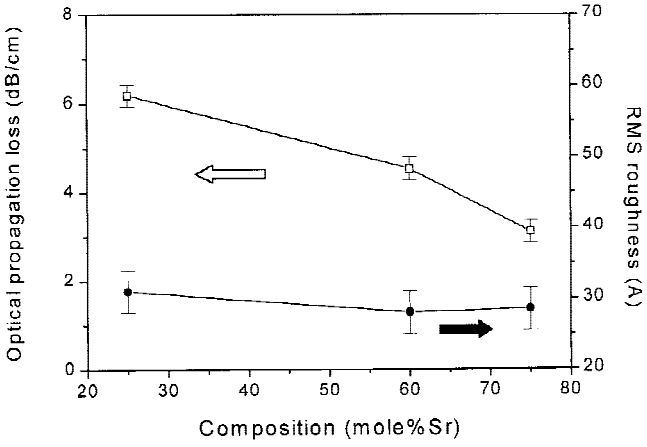

FIG. 11. Optical propagation loss and root-mean-square (rms) surface roughness of SBN thin films on SBN:25 composition seeded MgO substrates as a function of film composition.

up a continuous film into single-crystal islands by pores initially contained in the film. Thicker film was prepared by spin-coating to produce an epitaxial film via grain growth from the seeded islands. Compared with the film on an unseeded substrate, the film on a seeded substrate had high orientation because the number of epitaxial nuclei increased at the interface between the film and the substrate. The lower the Sr content in the film, the better epitaxial growth we could obtain. This was because the unit-cell network distorted and the lattice parameters of the SBN thin film changed. To obtain highly oriented film with high Sr content, SBN:75 film was prepared on MgO substrate with SBN:25 composition seeds layer. The anisotropy of the refractive indices of films decreased certainly as the Sr content in the film increased. Because of the low birefringence of the refractive indices, the optical scattering by the anisotropy of refractive indices was suppressed. As a result, that the optical propagation loss of the film decreased with an increase of the Sr content, though the rms surface roughness was constant regardless of the film composition. Since the sol-gel method enabled the fabrication of micro-devices with varied and complex shapes, the sol-gel-derived SBN thin films with excellent structural and optical properties could be important materials for optical waveguide applications.

ACKNOWLEDGMENTS

This work was financially supported by Korea Science and Engineering Foundation, under Grant No. 981-0803-019-2, and partly by the Brain Korea 21 project.

REFERENCES

1. A.M. Glass, J. Appl. Phys. **40,** 4699 (1969).
2. R.R. Neurgaonkar, W.F. Hall, J.R. Oliver, W.W. Ho, and W.K. Cory, Ferroelectrics **87,** 167 (1988).
3. P.V. Lenzo, E.G. Spencer, and A.A. Ballman, Appl. Phys. Lett. **11,** 23 (1967).
4. Y. Xu, C.J. Chen, R. Xu, and J.D. Mackenzie, Phys. Rev. B **44,** 35 (1991).
5. N.S. VanDamme, A.E. Sutherland, L. Jones, K. Bridger, and S.R. Winzer, J. Am. Ceram. Soc **74,** 1785 (1991).
6. S.S. Thöny, K.E. Youden, J.S. Harris, Jr., and L. Hesselink, Appl. Phys. Lett **65,** 2018 (1994).
7. M. Lee, and R.S. Feigelson, J. Crystal Growth **180,** 220 (1997).
8. W. Sakamoto, T. Yogo, K. Kikuta, K. Ogiso, A. Kawase, and S. Hirano, J. Am. Ceram. Soc. **79,** 2283 (1996).
9. C.H. Luk, C.L. Mak, and K.H. Wong, Thin Solid Films **298,** 57 (1997).
10. A.Y. Oral and M.L. Mecartney, J. Mater. Res. **15,** 1417 (2000).
11. K.T. Miller, F.F. Lange, and D.B. Marshall, J. Mater. Res. **5,** 157 (1990).
12. W.M. Cane, J.P. Spratt, and L.W. Hershinger, J. Appl. Phys. **37,** 2085 (1966).
13. J.H. Kim and F.F. Lange, J. Mater. Res **14,** 1626 (1999).
14. A. Seifert, A. Vojta, J.S. Speck, and F.F. Lange, J. Mater. Res. **11,** 1470 (1996).
15. J. Koo, J.H. Jang, and B-S. Bae, J. Am. Ceram. Soc. (in press).
16. J. Koo, S-U. Kim, D.S. Yoon, K. No, and B-S. Bae, J. Mater. Res. **12,** 812 (1997).
17. W-J. Lee and T-T. Fang, J. Am. Ceram. Soc. **81,** 193–199 (1998).
18. C.K. Baringay and S.K. Dey, Appl. Phys. Lett. **61,** 1278 (1992).
19. M.P. Trubelja, E. Ryba, and D.K. Smith, J. Mater. Sci. **31,** 1435 (1996).
20. J. Koo, C. Lee, J.H. Jang, K. No, and B-S. Bae, Appl. Phys. Lett **76,** 2671 (2000).
21. L. Venturini, E.G. Spencer, P.V. Lenzo, and A.A. Ballman, J. Appl. Phys. **39,** 343 (1968).
22. D.K. Fork, F. Armani-Leplingard, J.J. Kingston, and G.B. Anderson, in *Thin Films for Intergated Optics Applications,* edited by B.W. Wessels, S.R. Marder, and D.M. Walba (Mater. Res. Soc. Symp. Proc. **392,** Pittsburgh, PA, 1995), p. 189.